Biosensors and Bioelectronics 126 (2019) 200–206

Contents lists available at ScienceDirect

Biosensors and Bioelectronics

journal homepage: www.elsevier.com/locate/bios

A rapid real-time quantification in hybrid paper-polymer centrifugal optical devices

SeJin Kim, Dami Kim, Sanghyo Kim*

Department of Bionanotechnology, Gachon University, Seongnam 461-701, Republic of Korea

ARTICLE INFO

Keywords:
Colorimetric
Centrifugal
Glucose
Optical
Paper
Real-time

ABSTRACT

The research progress in the centrifugal microfluidic platform provides great opportunities for simple and effective analytical measurements in a variety of areas including biomedical engineering. In this study, we propose an optical reader that can measure the transmittance in a very sensitive and rapid manner on a hybrid paper-polymer centrifugal disc platform. This device enables real-time monitoring of multiple samples by measuring the absorbance of the light transmitted through the paper integrated on the disc between the light emitting diode (LED) and the photodiode (PD) regardless of the ambient light condition. To confirm its efficiency, we analyzed one of the blood's important indicators, glucose in a successful manner within 10 s without any additional complex image analysis. In addition, we discussed the results by comparing with the reflectance-based methods and with those of the previously reported studies by introducing a figure of merit to evaluate the performance of the assay.

1. Introduction

Currently, paper microfluidic devices have great potential point-of-care (POC) diagnostics due to their advantages such as low-cost, simple fabrication, easiness to dry biological samples, surface functionalization, and passive transport of fluids without an external pump (Ahmed et al., 2016; Akyazi et al., 2018; Morbioli et al., 2017). However, there are few limitations, including flow control, valving and metering that are possible on other microfluidic platforms. To overcome these limitations, several studies are in progress to demonstrate the integration of paper elements within a centrifugal microfluidic platform (Godino et al., 2014; Hwang et al., 2011; Kinahan et al., 2015; Vereshchagina et al., 2013; Wiederoder et al., 2017). In general, centrifugal microfluidics or lab-on-a-disc device relies on an automated rotating motor to manipulate fluid flow in the channel using centrifugal force (Gorkin et al., 2010; Strohmeier et al., 2015). Moreover, the integration of paper elements not only helps to improve the assay performance due to their unique porous 3D network and surface chemistry, but also offers opportunities such as bi-directional fluid control, valving, and metering. However, one of the big challenges with the centrifuge platform is the signal detection, which is inherently required. Most reports do not generally detect the output signal while the disc is in spinning.

At present, colorimetric methods combined with paper substrates have been attracting much attention as the results can be quickly visualized without any sophisticated equipment (Santana-Jiménez et al., 2018; Zhang et al., 2016; Zhu et al., 2014). However, colorimetric changes that make visual interpretation is a difficult task and necessitates the development of new methods for data acquisition. In many studies, the light reflectance-based analysis was performed using a line scanner, charge coupled device (CCD), complementary metal-oxide semiconductor (CMOS) image sensor, or smartphone camera to improve the objectivity of the results in a quantitative manner (Chen et al., 2012; Gabriel et al., 2017; Ortiz-Gómez et al., 2018; Wang et al., 2016; T. Wang et al., 2017). However, since the thickness of a commonly used paper is in the range of 50–400 μm, the light reflectance-based method, which obtains information only from the light absorbing particles existing in the upper 10–20 μm may limit the significant sensitivity (Ellerbee et al., 2009; Swanson et al., 2015). In addition, other important factor in the accurate analysis of results is color uniformity (Evans et al., 2014b). To improve color uniformity, various strategies of enzyme immobilization or modification of paper into nanomaterials have been reported. However, they are not easily available due to enzyme inactivation and complicated experimental procedures (de Tarso Garcia et al., 2014; Evans et al., 2014a; Figueredo et al., 2015; Gabriel et al., 2016; Wang et al., 2018; Yetisen et al., 2013). Moreover, as the high surface area is inherent in the paper, small amounts of the analytical sample solution can evaporate very quickly and affect the results of the colorimetric analysis. Therefore, the paper should be uniformly

* Corresponding author.
E-mail address: samkim@gachon.ac.kr (S. Kim).

https://doi.org/10.1016/j.bios.2018.10.064
Received 27 September 2018; Received in revised form 30 October 2018; Accepted 30 October 2018
Available online 31 October 2018
0956-5663/

wetted for at least till the detection. However, many studies have performed endpoint detection methods without considering liquid evaporation, which affects measurement in enzyme-based colorimetric reactions.

To overcome these technical challenges, we developed hybrid paper-polymer centrifugal optical devices. With the developed device, light absorbing particles can be detected over the entire thickness of a paper by measuring light transmittance with accuracy and high sensitivity compared to light reflectance measurement. Furthermore, the controlled fluid flow by centrifugal force can enhance reproducibility and uniformity of color since samples are injected simultaneously into multiple detection zones with the same force. Additionally, simultaneous sample injection allows all reactions to start at the same time, which provides an opportunity for analysis of enzyme kinetics. Therefore, results can be delivered within few seconds before the paper is dried through real-time colorimetric monitoring. As a proof of concept, we have successfully performed simultaneous detection of glucose at different concentrations. In this paper, we describe the technology of hybrid paper-polymer centrifugal optics system and present a rapid quantification platform with high sensitivity, uniformity, and real-time detection through enzyme-based glucose colorimetric assay. A comparison of analytical performance of the present method with previously reported detection methods were also presented.

2. Experimental

2.1. System design and fabrication

In this study, real-time quantitative glucose assays were optimized through the integration of hybrid paper-polymer discs, optoelectronic devices, and enzymatic assays. For this, the hybrid paper-polymer disc was placed between two electronic circuits designed to measure light transmittance through the paper. The acrylic case (140 × 110 × 32 mm) was manufactured using a milling machine (COMCON, CM-3525) to completely block the influence of external light sources and align two optical devices (LED and photodiode) and the detection zone on the disc (Fig. 1a). The device design is shown in Fig. S1.

2.1.1. Hybrid paper-polymer disc design and fabrication

The hybrid paper-polymer centrifugal disc (radius = 45 mm, thickness = 1.2 mm) was assembled from the standard black compact disc, laminating film (thickness = 100 μm) and cellulose chromatography paper (Whatman, 3MM Chr, thickness = 340 μm). The fabricated hybrid paper-polymer centrifugal disc has detection zones (5 × 3 mm), inlet channels (7 × 1 mm) and reference hole (diameter = 3 mm) as illustrated in Fig. 1b. The black acrylic paint was applied to the disc surface to minimize light scattering and loss. Laminating film and chromatography paper were cut based on the shape and size of the disc using a CO_2 laser marking machine (DONGIL, MC30). For disc assembly, the laminating film was attached firmly to the bottom of the disc using a hot press (Ocean Science, South Korea) and chromatography paper was placed on each detection zone.

2.1.2. Electronics

The photodiode (OSRAM, SFH2440) (λ_{max} = 620 nm) is a transducer that converts received light into a current signal. A transimpedance amplifier circuit (I-V converter) was used to convert and to amplify current signal into a voltage. The amplifier (TEXAS INSTRUMENTS, OPA2376) has rail-to-rail, low power, low input bias current with low noise and low offset characteristics and was chosen to reduce errors due to offset and 1/f noise while maintaining low power consumption. The output voltage of the PD transimpedance amplifier circuit was converted to digitized voltage with a 16-bit analog-digital converter (ADC) (LINEAR TECHNOLOGY, LTC1859) and transmitted to the computer using UART communication (Fig. 1c). The ADC sampling rate was set sufficiently faster than the Nyquist rate to recover the pulsed data with a high temporal resolution. A LED (Samsung Electro-Mechanics, SLSNNGA825TS) (λ_{max} = 520 nm, green) is used as a light source, which emits light in proportion to the flowing current, and the efficiency of light emission changes due to heat generation when driven by voltage (Bui and Hauser, 2015). As a result, a stable light source can be secured by using the constant current LED driver circuit. The fabricated PD transimpedance and constant current LED driver circuit board are shown in Figs. S2 and S3, respectively. The DC motor (Mabuchi motor, RF-300FA-11420) was able to mount the disc easily by the products used in general CD/DVD-ROM. Pulse width modulation (PWM) technology and a motor driver circuit (TEXAS INSTRUMENTS, DRV8838) were used for controlling the rotational speed of the motor. All circuits were controlled using the Arduino Uno 8-bit microcontroller and all systems were powered using a lithium polymer battery.

2.1.3. Assay procedures

D-(+)-Glucose, glucose oxidase (GOD) (100 U/mg), peroxidase (POD) (250 U/mg), 4-aminoantipyrine (4-AAP), sodium 3,5-dichloro-2-hydroxybenzenesulfonate (DHBS), D-(+)-trehalose dihydrate (≥98.5%) and phosphate buffered saline powder (10 mM, pH 7.4) were purchased from Sigma-Aldrich. All chemicals were used as received and prepared with ultrapure water (18 MΩ cm, Millipore) without further purification. For glucose assay, the enzymatic method was based on the Trinder's reaction (Fig. 1d). The glucose assay was realized using a mixture of GOD (100 U/mL) and HRP (250 U/mL) prepared in 0.3 M trehalose in phosphate buffered saline (trehalose-PBS) and PBS (pH = 7.4). Chromogen solutions (4-AAP (40 mM) and DHBS (40 mM)) were dissolved in water respectively. All solutions were stored in the refrigerator until analysis time. Enzyme and chromogen (assay reagent) were freshly mixed in a 1:1:1:1 ratio, after which 5uL of assay reagent was spotted on each detection zone and perfectly dried for 2 h in the dark environment. Working solutions of glucose (2.5–400 mg/dL) were prepared from a stock solution of 400 mg/dL in water. Finally, working solutions containing glucose (4 μL) were introduced into each inlet channel and allowed to reach the detection zones by centrifugal force. All reactions were performed at room temperature.

2.2. Data acquisition and analysis

2.2.1. Hybrid paper-polymer centrifugal optical devices

All data were stored as a comma separated value (CSV) extension file using the serial-oscilloscope free software (http://x-io.co.uk/serial-oscilloscope/). The plot shown in Fig. S4 can be obtained when the device operates. Each time the disc rotates, 19 pulses are generated continuously. Due to the disc reference hole (without paper), one pulse has the maximum ADC output value (2^{16}–1 = 65,535) of the 16-bit ADC and is used as the reference value for data alignment. Peak values of each pulse were extracted and aligned using a programming language, Visual Basic for Applications (VBA) to obtain real-time absorbance for each detection zone. The aligned peak values were converted to absorbance values using Eq. (1), where N (1–19) is the number of the detection zone and M (≥35) is the cycle number. Therefore, as the colorimetric reaction proceeds, the light source is blocked, so that the denominator of Eq. (1) decreases and the absorbance increases. In this way, colorimetric reactions of 18 detection zones can be monitored in real time. In this paper, we collected data from the 35th cycle as a starting point (See Section 3.1.).

$$Absorbance_{Nth\ zone} = \log 10\left(\frac{ADC\ Value_{35th\ cycle},\ N\ th\ zone}{ADC\ Value_{Mth}\ cycle,\ N\ th\ zone}\right) \quad (1)$$

2.2.2. Reflectance measurement using a scanner

The reflectance was measured using a line scanner (HP Scanjet 200) and the scan was performed in color mode at a resolution of 2400 ×

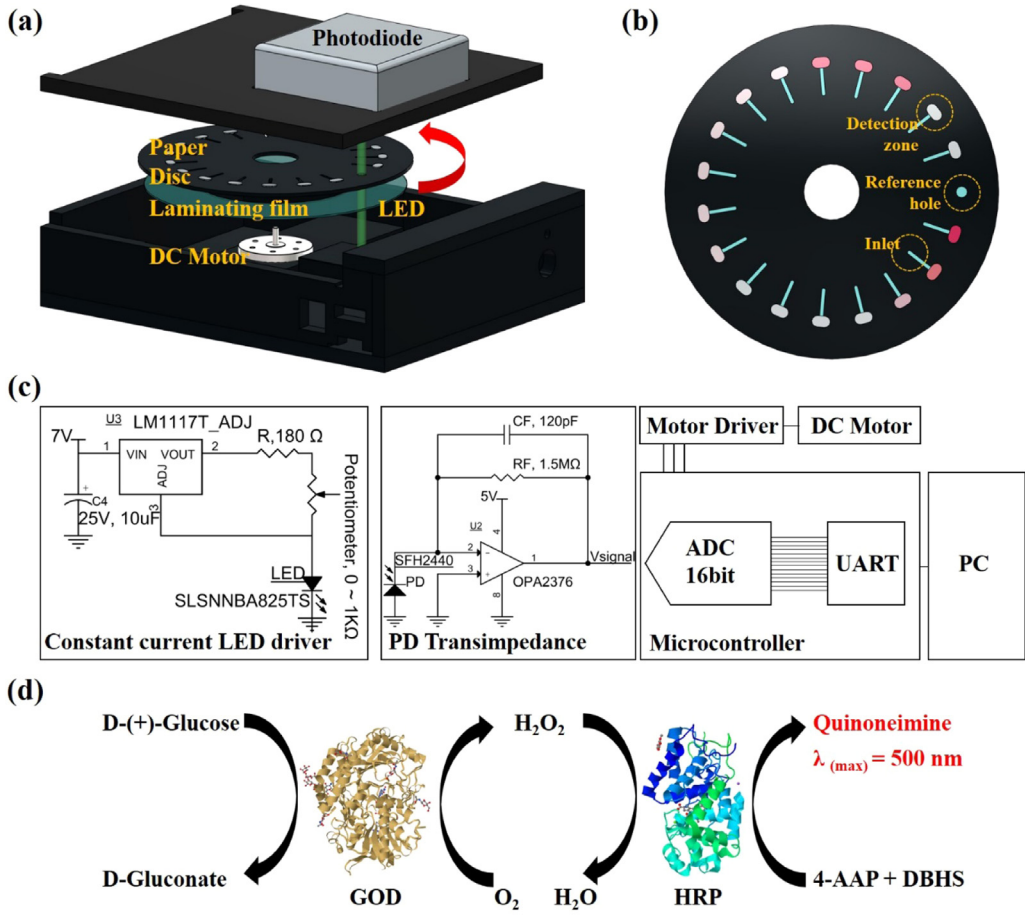

Fig. 1. (a) The manufactured acrylic case has a frame to mount the DC motor. The detection zone of the disc is aligned between the photodiode and the LED circuit. (b) Hybrid paper-polymer discs have 18 inlet channels and detection zones. It also has one reference hole for data sorting. (c) The constant current LED driver circuit is designed to adjust the brightness of the light source using a potentiometer. In photodiode transimpedance circuit, the photodiode is reverse biased, and the gain and bandwidth can be determined by feedback resistor (RF) and feedback capacitor (CF) values. The output voltage is digitized by 16-bit analog-digital converter (ADC) and transmitted to the PC via universal asynchronous receiver/transmitter (UART) communication. The microcontroller also controls the DC motor with pulse-width modulation (PWM). (d) Bienzymatic colorimetric glucose detection assay diagram.

4800 dpi (dots-per-inch). Images were saved as Tagged Image File Format (TIFF). Adobe Photoshop CS6 was used for image analysis and color extraction. Color extraction was performed using the eyedropper tool by averaging the color value with 102 × 51 pixels of each detection zone and by using the RGB color values for data analysis. Background white RGB value was obtained in a similar manner and used as a reference value of color difference value. The color difference was calculated using Eq. (2), where (R_2-R_1)is the red variation, (G_2-G_1) is the green variation, and (B_2-B_1)is the blue variation.

$$Color\ difference = \sqrt{(R_2-R_1)^2 + (G_2-G_1)^2 + (B_2-B_1)^2} \quad (2)$$

3. Results and discussion

3.1. Optimal data collection cycle decision

After loading 18 sample solutions into the inlet channels, the solution can be transferred to the paper by centrifugal force of the operating device. As the paper becomes wet (during 1.5 s), increased peak ADC values were observed due to higher light transmittance of the wetted paper than the dry paper (Fig. 2). The enzyme reaction started at 1.5 s, the time when the paper was completely wetted, and an additional 3.5 s also required to stabilize the peak ADC value. This is thought to be caused by the optical noise due to diffraction and refraction in the process of completely immersing the solution in the paper, and the radiation noise during deceleration of the brush DC motor. As a result, data analysis was performed after 35 cycles (5 s after device operation) as stable data and setting this cycle as default. After the start of the reaction, dead time (3.5 s) was present but did not significantly affect the analytical results. For convenience, the graph time axis that will be shown will start at 5 s (acceleration time + dead time). Also, A_T is the absorbance value at T seconds, and ΔA_T is defined as the linear regression slope for T seconds.

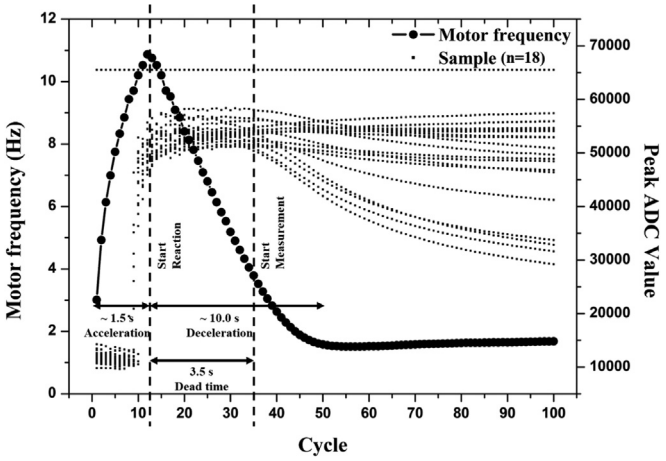

Fig. 2. Cycle versus motor rotation frequency and Peak ADC value of each detection zone.

3.2. Real-time glucose measurement

3.2.1. Effect of trehalose

Trehalose is a commonly used reagent for stabilizing enzymes and is known to protect the activity of the dried form of the enzyme (Curto et al., 2013; Evans et al., 2014b; Gabriel et al., 2016; Klasner et al., 2010; Paz-Alfaro et al., 2009). The enzyme solution (GOD, POD) was prepared in 0.3 M trehalose-PBS and PBS (pH = 7.4) to confirm the

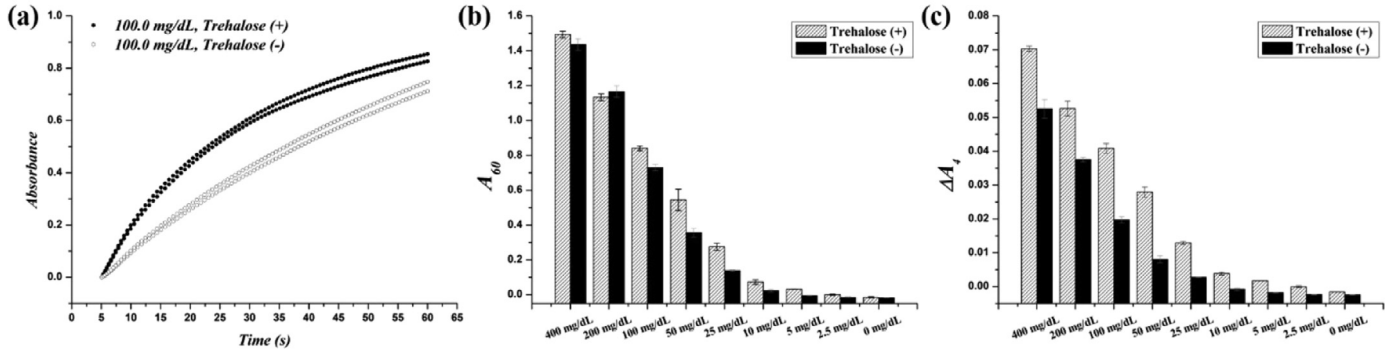

Fig. 3. Analytical performance of colorimetric based glucose assay with and without trehalose. (a) Absorbance graph for glucose (100 mg/dL) over time. (b) Absorbance at 60 s (A_{60}) for each concentration. (c) Linear regression slope (ΔA_4) for each concentration. All values represent the mean and standard deviation of two independent experiments.

effect of trehalose in the glucose assay. Various concentrations (2.5–400 mg/dL) of glucose solution were continuously monitored for 60 s Fig. 3a shows representative results of the trehalose effect at 100 mg/dL glucose concentration and Fig. S5 summarizes the results of other tested concentrations. As shown in Fig. 3b, trehalose does not significantly affect the A_{60} results. On the other hand, Fig. 3c shows that trehalose increases the initial reaction rate significantly. The obtained results were consistent with previous reports of the role of trehalose in increasing the initial rate (efficiency) of glucose oxidase (Paz-Alfaro et al., 2009). In this experiment, the device enabled the kinetic analysis of the enzyme through real-time data acquisition.

3.2.2. Calibration curve of glucose

After establishing optimal experimental conditions for assay, the glucose standard solution was appropriately diluted to generate a calibration curve in the concentration range of 2.5 mg/dL to 400 mg/dL. Absorbance over time was plotted and showed strong differentiation between the different glucose concentrations (Fig. 4a). Fig. 4b shows the absorbance graph for the initial 9 s. As can be seen from the graph, the absorbance at the blank (0 mg/dL) continues to decrease below zero. This is a result of the reduction of the path length due to the evaporation of the liquid layer on the paper, which had initially been wetted with sufficient solution. On the other hand, in the presence of glucose, the effect of net potential between color conversion and liquid evaporation showed a change in absorbance is sufficiently distinguishable from the blank. Fig. 4c and d show A_{60} and ΔA_4 graphs and in both graphs, the linear calibration curve were in the concentration range of 2.5–50 mg/dL. Fig. 4e shows the Pearson's correlation analysis results of A_{60} and ΔA_4. The correlation coefficient was 0.9974, which shows a very high positive correlation.

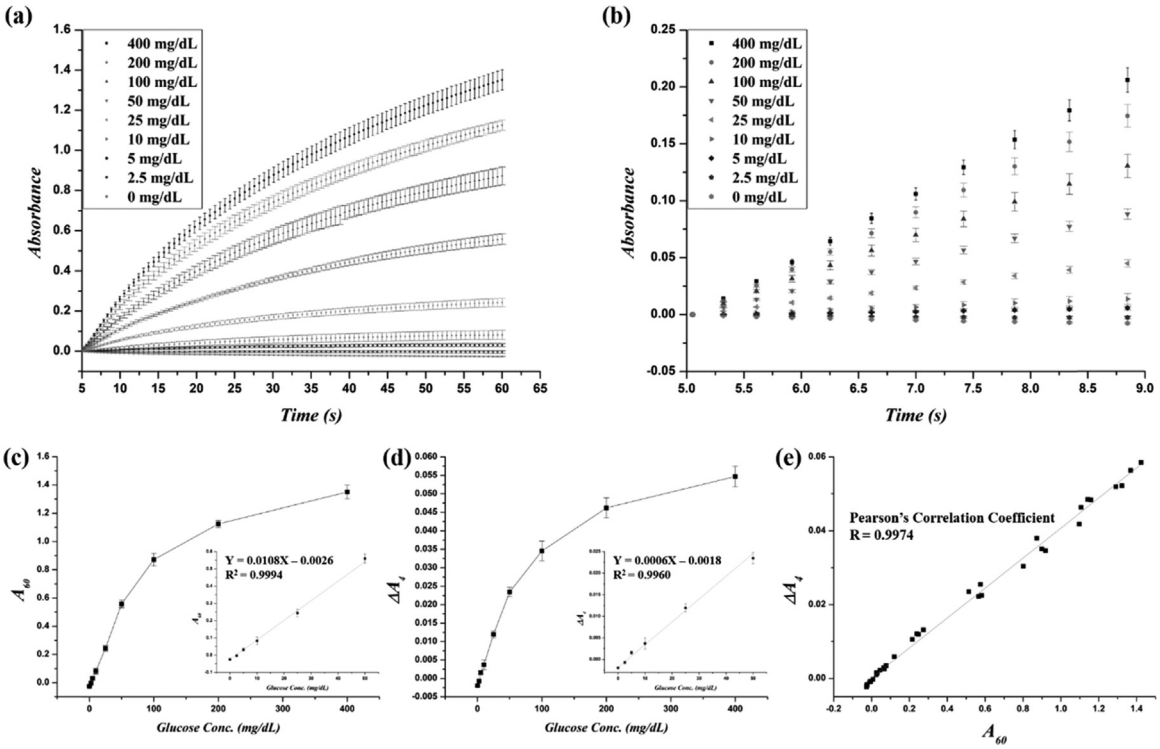

Fig. 4. Analytical curve of glucose. The graph for absorbance over time at various glucose concentrations (a) 60 s (b) 9 s (c) Absorbance at 60 s (A_{60}) for each concentration. The inset shows the linear calibration curve of glucose at the range of 2.5–50 mg/dL. (d) Linear regression slope (ΔA_4) for each concentration. The inset shows the linear calibration curve of glucose at the range of 2.5–50 mg/dL. (e) Pearson's correlation analysis and correlation coefficient. All values represent the mean and standard deviation of four independent experiments.

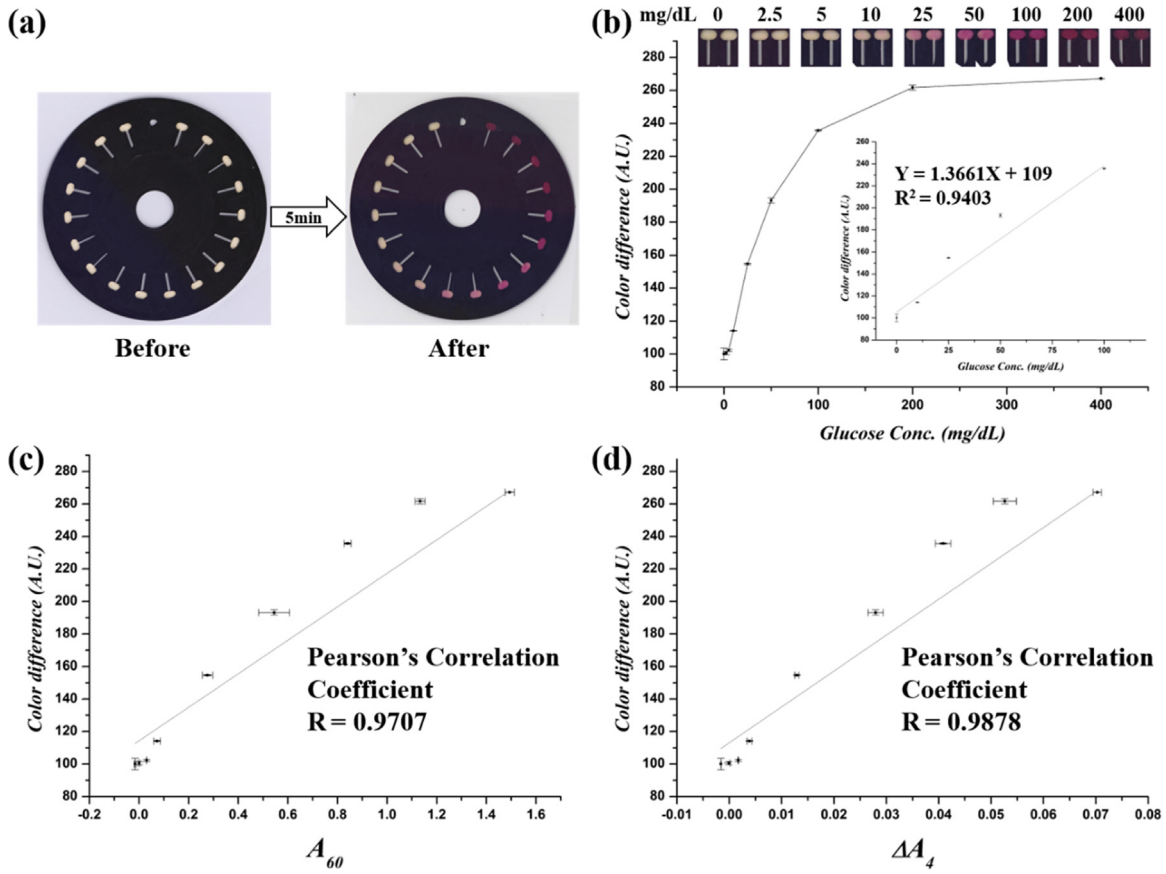

Fig. 5. (a) A digital image obtained using a scanner before and after the glucose reaction. (b) Image used for color extraction. The average color difference values and standard deviations are plotted for each glucose concentration. The inset shows the linear calibration curve of glucose at the range of 10–100 mg/dL. (c) A_{60} and color difference correlation graph and pearson correlation coefficient. (d) ΔA_4 and color difference correlation graph and pearson correlation coefficient. All values represent the mean and standard deviation of two independent experiments.

3.2.3. Comparison with reflectance-based measurements

To evaluate the performance of our transmittance-based device, we also compared it with the reflectance-based measurement method. Many studies have reported methods for quantifying colorimetric reactions based on reflectance by developing their image analysis algorithms using CCD, CMOS image sensors, smartphone cameras, and scanners (Chen et al., 2012; Gabriel et al., 2017; Ortiz-Gómez et al., 2018; Wang et al., 2016; T. Wang et al., 2017). However, when capturing images using these devices, the lighting conditions must be carefully adjusted. The external light source greatly affects the color intensity of the image, and a change in the lighting condition can cause a considerable variation in the colorimetric determination. Therefore, we used a scanner that can minimize the deviation from the external light source. To compare under the same conditions, after the real-time quantification experiment using centrifugal optical devices, we scanned the disc immediately and obtained an image.

Fig. 5a shows the scanned image before and after the glucose assay on the disc. We extracted the color difference with the scanner, and the linear calibration curve generated from 10 to 100 mg/dL (Fig. 5b). Fig. 5c, d shows the correlation analysis graph of A_{60} and ΔA_4 and color difference, respectively. Especially, it showed non-linearity at low concentration. Therefore, it can be proved that our device's transmittance measurement method is more sensitive than the reflectance-based measurement on a scanner.

3.3. Figures of merit

The endpoint measurement method is to measure the result after the substrate is exhausted with sufficient reaction time. It can be employed to minimize errors when simultaneous sample injection and real-time measurements are not available. On the other hand, because our devices are capable of simultaneous sample injection and real-time detection, the measurement results are not affected by the reaction time. Thus, we obtained all LODs between 5 and 60 s in absorbance (A_T) and linear regression slope (ΔA_T). The LOD was calculated using Eq. (3), where σ is the standard deviation of the reagent blank (where n = 10) and S is the slope of the calibration curve.

$$LOD = \frac{3.3(\sigma)}{S} \tag{3}$$

As can be seen in Fig. 6, the short time measurement shows a relatively high LOD. On the other hand, the longer the measurement time, the lower the LOD and converged to a constant value. This shows that there is a trade-off relationship between LOD and time to result. That is, a fast "time to result" bring about a deterioration in sensitivity, and a lot of time is required for high sensitivity. In biosensors and in diagnostics, time to result is an important factor to be considered just as LOD. Therefore, we have defined the reciprocal of the product of LOD and "time to result" as a new figure of merit to numerically interpret it. The figure of merit was generally higher in the linear regression slope (ΔA_T) method than the absorbance (A_T) method (Fig. 6). The optimal figure of merit were 0.1279 and 0.1560, respectively. And there, the LOD values of A_{11} and ΔA_{11} were 0.7418 mg/dL (41.18 μM) and 0.6080 mg/dL (33.75 μM), respectively. On the other hand, the lowest LOD was 0.4704 mg/dL (26.11 μM) in A_{33} and 0.3727 mg/dL (20.69 μM) in ΔA_{28}. The linear regression slope based measurements, which calculated from multiple data points, can provide in a shorter time with more resilient measurement results for reading errors and singular values.

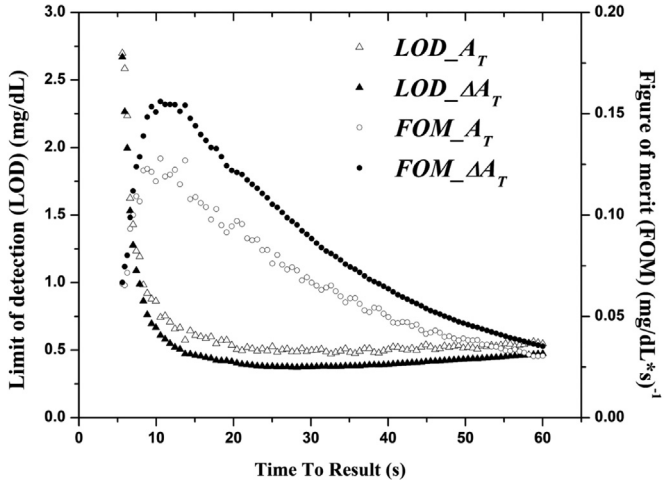

Fig. 6. Limit of detection (LOD) and Figure of merit (FOM) versus Time To Result.

Table S1 shows the LOD values in the colorimetric glucose detection studies performed on paper devices and the analytical data using the figure of merit suggested by us.

In addition, we extracted information on repeatability and reproducibility by comparing zone to zone and disc to disc. In terms of repeatability, the relative standard deviation (RSD) found for simultaneous analysis (n = 4) on a single disc were 3.96% and 3.78% in A_{60} and ΔA_4, respectively. On the other hand, the RSD values of the disc to disc (n = 8) were 6.97% and 6.92% in A_{60} and ΔA_4, respectively. According to the data, the proposed hybrid paper-polymer centrifugal optical devices can be inferred that provides excellent repeatability and reproducibility.

4. Conclusion

In conclusion, we have demonstrated that the concentration of glucose can be analyzed in real-time by the hybrid paper-polymer centrifugal optical device system through light transmission measurements. The real-time monitoring enables slope-based measurement and can provide results within a short time (maximum of 30 s) while maintaining high sensitivity. Under the optimal conditions, linear range was obtained in the range of 2.5–25 mg/dL with the detection limit of 0.3727 mg/dL, with excellent repeatability and reproducibility. Further, this sensing system may provide a cost-efficient, robust, and high-throughput opportunities for the simultaneous detection of multiple biological targets by simply adding reagents embedded in the paper depending on the application. In future, the hybrid paper-polymer centrifugal optical device system integrated with systems such as automated sample injector and meter, plasma separator (membrane) and microchannel will allow for real sample applications.

Acknowledgements

This research was supported by BioNano Health-Guard Research Center funded by the Ministry of Science and ICT of Korea as Global Frontier Project (Grant no. H-GUARD_2013M3A6B2078950 (ERND 1711072780)) and by the R&D Program for Society of the National Research Foundation (NRF) funded by the Ministry of Science and ICT of Korea (2015M3A9E2031372).

Competing financial interests

The authors declare no competing financial interests.

Appendix A. Supporting information

Supplementary data associated with this article can be found in the online version at doi:10.1016/j.bios.2018.10.064.

References

Ahmed, S., Bui, M.P., Abbas, A., 2016. Paper-based chemical and biological sensors: engineering aspects. Biosens. Bioelectron. 77, 249–263.
Akyazi, T., Basabe-Desmonts, L., Benito-Lopez, F., 2018. Review on microfluidic paper-based analytical devices towards commercialisation. Anal. Chim. Acta 1001, 1–17.
Bui, D.A., Hauser, P.C., 2015. Analytical devices based on light-emitting diodes–a review of the state-of-the-art. Anal. Chim. Acta 853, 46–58.
Chen, X., Chen, J., Wang, F., Xiang, X., Luo, M., Ji, X., He, Z., 2012. Determination of glucose and uric acid with bienzyme colorimetry on microfluidic paper-based analysis devices. Biosens. Bioelectron. 35 (1), 363–368.
Curto, V.F., Lopez-Ruiz, N., Capitan-Vallvey, L.F., Palma, A.J., Benito-Lopez, F., Diamond, D., 2013. Fast prototyping of paper-based microfluidic devices by contact stamping using indelible ink. Rsc Adv. 3 (41), 18811–18816.
de Tarso Garcia, P., Cardoso, T.M.G., Garcia, C.D., Carrilho, E., Coltro, W.K.T., 2014. A handheld stamping process to fabricate microfluidic paper-based analytical devices with chemically modified surface for clinical assays. Rsc Adv. 4 (71), 37637–37644.
Ellerbee, A.K., Phillips, S.T., Siegel, A.C., Mirica, K.A., Martinez, A.W., Striehl, P., Jain, N., Prentiss, M., Whitesides, G.M., 2009. Quantifying colorimetric assays in paper-based microfluidic devices by measuring the transmission of light through paper. Anal. Chem. 81 (20), 8447–8452.
Evans, E., Gabriel, E.F.M., Benavidez, T.E., Coltro, W.K.T., Garcia, C.D., 2014a. Modification of microfluidic paper-based devices with silica nanoparticles. Analyst 139 (21), 5560–5567.
Evans, E., Gabriel, E.F.M., Coltro, W.K.T., Garcia, C.D., 2014b. Rational selection of substrates to improve color intensity and uniformity on microfluidic paper-based analytical devices. Analyst 139 (9), 2127–2132.
Figueredo, F., Garcia, P.T., Cortón, E., Coltro, W.K., 2015. Enhanced analytical performance of paper microfluidic devices by using Fe3O4 nanoparticles, MWCNT, and graphene oxide. ACS Appl. Mater. Interfaces 8 (1), 11–15.
Gabriel, E., Garcia, P., Lopes, F., Coltro, W., 2017. Paper-based colorimetric biosensor for tear glucose measurements. Micromachines 8 (4), 104.
Gabriel, E.F., Garcia, P.T., Cardoso, T.M., Lopes, F.M., Martins, F.T., Coltro, W.K., 2016. Highly sensitive colorimetric detection of glucose and uric acid in biological fluids using chitosan-modified paper microfluidic devices. Analyst 141 (15), 4749–4756.
Godino, N., Vereshchagina, E., Gorkin, R., Ducrée, J., 2014. Centrifugal automation of a triglyceride bioassay on a low-cost hybrid paper-polymer device. Microfluidics Nanofluidics 16 (5), 895–905.
Gorkin, R., Park, J., Siegrist, J., Amasia, M., Lee, B.S., Park, J.M., Kim, J., Kim, H., Madou, M., Cho, Y.K., 2010. Centrifugal microfluidics for biomedical applications. Lab Chip 10 (14), 1758–1773.
Hwang, H., Kim, S.H., Kim, T.H., Park, J.K., Cho, Y.K., 2011. Paper on a disc: balancing the capillary-driven flow with a centrifugal force. Lab Chip 11 (20), 3404–3406.
Kinahan, D.J., Kearney, S.M., Faneuil, O.P., Glynn, M.T., Dimov, N., Ducrée, J., 2015. Paper imbibition for timing of multi-step liquid handling protocols on event-triggered centrifugal microfluidic lab-on-a-disc platforms. RSC Adv. 5 (3), 1818–1826.
Klasner, S.A., Price, A.K., Hoeman, K.W., Wilson, R.S., Bell, K.J., Culbertson, C.T., 2010. Paper-based microfluidic devices for analysis of clinically relevant analytes present in urine and saliva. Anal. Bioanal. Chem. 397 (5), 1821–1829.
Morbioli, G.G., Mazzu-Nascimento, T., Stockton, A.M., Carrilho, E., 2017. Technical aspects and challenges of colorimetric detection with microfluidic paper-based analytical devices (muPADs) - a review. Anal. Chim. Acta 970, 1–22.
Ortiz-Gómez, I., Salinas-Castillo, A., García, A.G., Álvarez-Bermejo, J.A., de Orbe-Payá, I., Rodríguez-Diéguez, A., Capitán-Vallvey, L.F., 2018. Microfluidic paper-based device for colorimetric determination of glucose based on a metal-organic framework acting as peroxidase mimetic. Microchim. Acta 185 (1), 47.
Paz-Alfaro, K.J., Ruiz-Granados, Y.G., Uribe-Carvajal, S., Sampedro, J.G., 2009. Trehalose-mediated thermal stabilization of glucose oxidase from Aspergillus niger. J. Biotechnol. 141 (3–4), 130–136.
Santana-Jiménez, L.A., Márquez-Lucero, A., Osuna, V., Estrada-Moreno, I., Dominguez, R.B., 2018. Naked-eye detection of glucose in saliva with bienzymatic paper-based sensor. Sensors 18 (4), 1071.
Strohmeier, O., Keller, M., Schwemmer, F., Zehnle, S., Mark, D., von Stetten, F., Zengerle, R., Paust, N., 2015. Centrifugal microfluidic platforms: advanced unit operations and applications. Chem. Soc. Rev. 44 (17), 6187–6229.
Swanson, C., Lee, S., Aranyosi, A., Tien, B., Chan, C., Wong, M., Lowe, J., Jain, S., Ghaffari, R., 2015. Rapid light transmittance measurements in paper-based microfluidic devices. Sens. Bio-Sens. Res. 5, 55–61.
Vereshchagina, E., Bourke, K., Meehan, L., Dixit, C., Mc Glade, D., Ducrée, J., 2013. Multi-material paper-disc devices for low cost biomedical diagnostics. In: Proceedings of the 26th International Conference on Micro Electro Mechanical Systems (MEMS), IEEE, pp. 1049–1052.
Wang, T., Devadhasan, J.P., Lee, D.Y., Kim, S., 2016. Real-time DNA amplification and detection system based on a CMOS image sensor. Anal. Sci. 32 (6), 653–658.
Wang, T., Kim, S., An, J.H., 2017b. A novel CMOS image sensor system for quantitative loop-mediated isothermal amplification assays to detect food-borne pathogens. J. Microbiol. Methods 133, 1–7.
Wang, X., Li, F., Cai, Z., Liu, K., Li, J., Zhang, B., He, J., 2018. Sensitive colorimetric assay for uric acid and glucose detection based on multilayer-modified paper with

smartphone as signal readout. Anal. Bioanal. Chem. 410 (10), 2647–2655.
Wiederoder, M., Smith, S., Madzivhandila, P., Mager, D., Moodley, K., DeVoe, D., Land, K., 2017. Novel functionalities of hybrid paper-polymer centrifugal devices for assay performance enhancement. Biomicrofluidics 11 (5), 054101.
Yetisen, A.K., Akram, M.S., Lowe, C.R., 2013. Paper-based microfluidic point-of-care diagnostic devices. Lab Chip 13 (12), 2210–2251.
Zhang, Y., Gao, D., Fan, J., Nie, J., Le, S., Zhu, W., Yang, J., Li, J., 2016. Naked-eye quantitative aptamer-based assay on paper device. Biosens. Bioelectron. 78, 538–546.
Zhu, W.-J., Feng, D.-Q., Chen, M., Chen, Z.-D., Zhu, R., Fang, H.-L., Wang, W., 2014. Bienzyme colorimetric detection of glucose with self-calibration based on tree-shaped paper strip. Sens. Actuators B: Chem. 190, 414–418.